Numerical modeling of tunneling effects on adjacent structures

N. M. Saleh , W. A. Dawood, A. M. Elleboudy
Benha University, Faculty of Engineering at Shobra , Cairo, Egypt

ABSTRACT: The prediction of tunnel induced building deformation becomes a key issue in tunnel construction process. Current design approaches are conservative and lead to unnecessary expenditure in the design and construction of protective measures. This paper introduces a three dimensional elasto-plastic finite difference model to predict building damage due to tunnel construction taking into account the interaction between building stiffness, tunnel and the soil to refine the prediction of tunnel induced building deformation by generating settlement prediction/building damage assessment charts. These charts can be incorporated in the current damage risk assessment and may reduce the number of buildings for which an expensive, detailed evaluation has to be performed. Ground surface deformation and strains induced in building was investigated and compared with field measurement of two case studies; a building due to the construction of Greater Cairo Metro Line3-Phase1, and Neptune House due to the construction of the Jubilee line extension tunnel. Reasonable agreement was found between the observed field measurements and the predicted results using the 3D numerical simulation.

1 INTRODUCTION

Ground movements are an inevitable consequence of excavating and constructing a tunnel. Tunnel excavation causes relaxation of in-situ stresses, which are only partially restricted by the insertion of the tunnel support. Practically, it is not possible to create a void instantaneously and provide an infinitely stiff lining to fill it exactly. Hence, a certain amount of the ground deformation will take place at the tunnel depth. This will trigger a chain of movements, resulting in settlements at the ground surface, which become more significant with the decrease in tunnel depth. Several methods have been developed and used for the prediction of building induced settlement and the associated damage due to tunneling (Rankin 1988, Leblais et al. 1995, Mair et al. 2001, Franzius 2003, Pickhaver 2006). This paper introduces settlement prediction/building damage assessment charts (SP/BDA Charts) which can be used to estimate the main building settlement control parameters and preliminary assess the category of damage of the building due to tunnel induced subsidence. These charts were created by a verified finite difference model (FDM) using FLAC^{3D} program. The applicability and validity of these charts were examined and compared with two cases simulated numerically in FLAC^{3D} program.

2 FLAC^{3D} MODEL

2.1 *Mesh dimensions*

For the choice of sufficient mesh dimensions, stresses at the model boundaries should not be influenced by the tunnel excavation. The recommended mesh size is (4 to 5) x D (the tunnel diameter) from the tunnel centerline to the vertical mesh boundaries and (2 to 3) x D from the tunnel centerline to the bottom horizontal boundary (Moller 2006).

2.2 *Building*

The building was modeled by an elastic weightless shell located on the ground surface. It had a Young's modulus E_{eq}, and an equivalent thickness t_{eq}. For a building with N_s storey, the properties of the elastic shell were calculated assuming that the building consists of (N_s +1) slab with a vertical spacing of H_s

and thickness of slab t_s. With L being the length of the slab, the second moment of area I_{slab} and the area A_{slab} are defined as:

$$I_{slab} = \frac{t_s^{\,3} L}{12} \quad (1)$$

$$A_{slab} = t_s L \quad (2)$$

Using the parallel axis theorem (Timoshenko 1955) assuming the neutral axis to be at the mid-height of the building, the second moment of area for the equivalent shell was then calculated as follows:

$$(E_c I)_B = E_C \sum_{1}^{Ns+1} (I_{slab} + A_{slab} H_s^{\,2}) \quad (3)$$

$$(E_c A)_B = (N_s + 1)(E_c A_{slab}) \quad (4)$$

$$t_{eq} = \sqrt{\frac{12(E_c I)_B}{(E_c A)_B}} \quad (5)$$

$$E_{eq} = \frac{(E_c A)_B}{t_{eq}} \quad (6)$$

where E_c is he concrete Young's modulus, $(E_c\ I)_B$ is the building bending stiffness, A is the building cross sectional area, and $(E_c\ A)_B$ is the building axial stiffness. The input parameters for the shell elements used in the SP/BDA Charts are t_{eq}, E_{eq} and Poisson's ratio (ν) of 0.15.

2.3 *Boundary conditions*

For the vertical boundaries at the nodes, the vertical displacement (u_v) is left free and the horizontal displacement (u_h) is restrained allowing only for a normal stress (σ) and no shear stress (τ). For the bottom mesh horizontal boundaries at the nodes, the vertical displacement and both horizontal displacements are restrained, for the upper horizontal boundary, all nodes are left free to displace.

2.4 *Initial stress conditions*

A set of stresses representing soil initial state of stresses were installed in the grid, and then FLAC^{3D} is run until an equilibrium state is obtained. The initial horizontal stress is related to the initial vertical stress by at rest lateral earth pressure coefficient (K_0) which equals to (1-sinø), where ø is the angle of internal friction of the soil. It is worth noting that the soil mass is assumed to be dry and ground water is not considered in this study.

2.5 *Material model*

An elastic perfectly plastic Mohr-Coulomb material model was used to simulate the soil behavior.

2.6 *Tunnel construction*

The modeling of a tunnel excavation should ideally be a continuous process to simulate the construction of a real tunnel. All elements in the soil block, including those representing the interior of the tunnel and the lining, are soil elements. At each tunnel construction stage, installation of pre-support concrete, soil excavation and final lining installation were modelled. The installation of pre-support concrete was used to simulate the installation of face support, shotcrete (if any), and to obtain the required volume loss when the soil excavation was done. The numerical simulation of the pre-support concrete installation was done by installing a cylindrical shell around the excavated area with length equal to the excavation step length (L_{exc}) of 3.0m with isotropic properties as given in Table 1.

Table 1. Summary of lining properties.

Case	Density (kg/m^3)	Thickness (m)	E (GPa)	ν -
VCI*	2500	0.4	23	0.2
VCII**	2500	0.25	23	0.2
SP/BDA	2500	0.25	23	0.2

VCI* Greater Cairo Metro Verification Case
VCII** Jubilee Line Extension Verification Case

Modeling of soil excavation was achieved by the removal from the overall mesh the elements representing the interior of the tunnel by assigning null zone properties. After the soil was excavated the mesh is left to displace till a specific volume loss was achieved. After tunnel excavation, a final concrete lining was installed by activating a hollow cylinder zone with thickness equal to the tunnel final lining. The final tunnel concrete lining was modeled with zones, because FLAC^{3D} zones provide a reasonable approximation for bending of thick liners. The material properties used for the final concrete lining was the same which was used for the pre-support concrete, noting that full bond between tunnel lining and the surrounding soil was assumed.
The approach stated above for tunnel construction process retains the principal advantages of three dimensional simulation with reduced overall complexity of the model. Of course this relatively simple modelling procedure has the consequence that the level of detail provided for tunnel process was reduced. Also, the procedure is only appropriate for buildings on shallow foundations with no ground water.

3. MODEL VERIFICATION

The intent of this section is to verify the proposed FDM, to examine its applicability to be used as a predictive tool, and to show that it could be used for the derivation of the SP/BDA charts. Two cases were studied; the response of a building, located in Cairo, Egypt to the construction of Greater Cairo Metro Line 3-Phase 1 (From Attaba to Abbassia), and Neptune house response to the construction of the Jubilee Line Extension Tunnel in London.

3.1 *Greater Cairo Metro Line 3- Phase 1 case*

Greater Cairo underground metro consists of three lines linking the captial districts with the center of the city (Fig. 1). For this research study, the behavior and response of the chosen building was studied numerically using the proposed FDM and verified with the observed field data. This work has demonstrated the validity of certain techniques for modelling tunnel construction and its effects on adjacent buildings. The results was uutilized to derive the SP/BDA Charts. Monitoring of this site was carried out in January 2009 and extended to April 2009 during the advance of the TBM adjacent to the multi-storey building.

Figure 1. Greater Cairo metro lines.

3.1.1 *Ground conditions*

A detailed soil investigation was carried out prior to tunnel construction, including rotary coring and sampling for laboratory testing, piezometer tests, and standard penetration tests (NAT 2007). The ground formation at the section of the tunnel near the studied building was described in Table 2.

Table 2. Summary of main soil properties.

Layer	Thickness (m)	γ (kN/m^3)	ø	E (Mpa)
Fill	2.5	17	27	4
Upper sand	5.5	19.5	36	40
Middle sand	12.8	19.5	38	70
Sand-Gravel	1.3	20	41	200
Lower sand	-	19.5	38	240

3.1.2 *Description of the building*

The selected building is an old residential, 4-story, masonry wall bearing structure, shown in Figure 2. It is located at the intersection of Abd Elhalim Elzeini Street and Abbasia Street, Cairo, Egypt.

Figure 2. The selected building.

The building has approximate dimensions of 20m (parrallel to tunnel axis) and 26m (perpendicular to tunnel axis). Its facade is located at a distance of 8 m from tunnel centerline (Fig. 3). The depth of the tunnel axis is -22.5m.

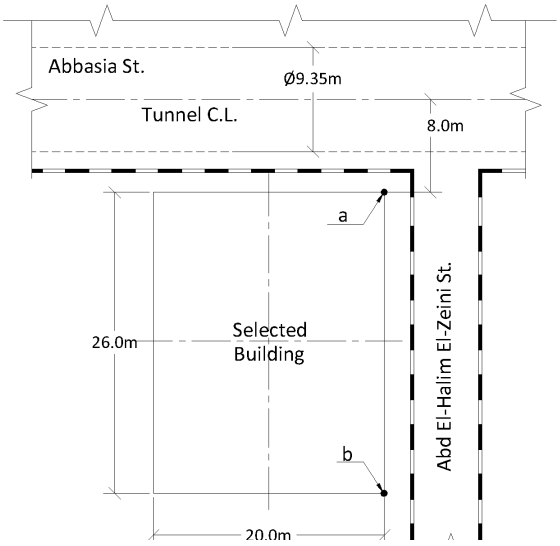

Figure 3. Layout showing the location of settlement points.

The choice of this building as a case study from a range of buildings was made based on certain criteria that served the objectives of the current research, taking into consideration the type of numerical methods to be validated. These criteria included that the building should be a wall bearing masonry structue, with no cracks or distresses before tunnel construction, building orientation is nearly perpendicular to tunnel route, built on simple strip or spread footings, and unprotected by compensation grouting as modelling of this protection method is not a part of this research. The studied building had satisfied all the above criteria. The foundation level is approximately at -2.5 m. The roof slab thickness is 0.15m. The ground floor height is approximately 3.6m and typical floors height is approximately 3.2m.

3.1.3 *Tunnel induced settlement*

From the monitring measurements report (NAT 2009) submitted by the contarctor to National Authority for Tunnels in March 2009, the maximum vertical movement of point **a** (shown in Fig. 3) was 3.0mm, and the maximum vertical movement for Point **b** was 1.0mm. These readings was recorded after the Tunnel Boring Machine had passed the building with a distance of 215.25m, and duration of 20 days.

3.1.4 *Finite difference numerical model composition*

Soil was modeled using a mesh with dimensions of 120m in width, 120m in length and 60m in height (Fig. 4).

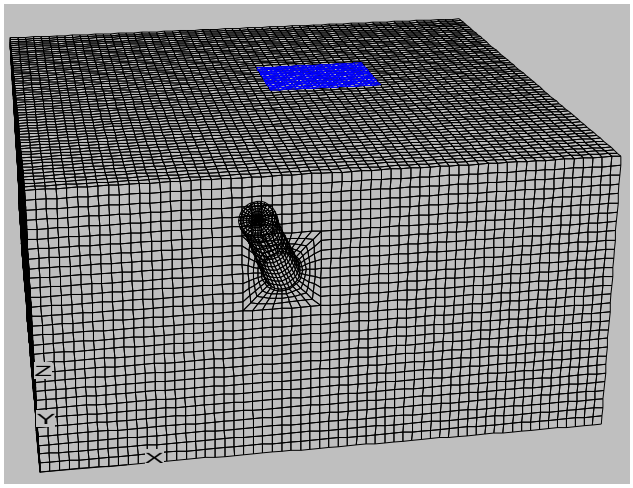

Figure 4. Mesh geometry for Greater Cairo Metro case study.

The building was modeled by an elastic weightless shell located on the ground surface. It had a length of 20m, a width of 26m, and the horizontal distance between its nearest edge and the tunnel centerline was 8.0m. The tunnel was modeled as cylindrical element at depth of 20.0m from ground surface.

Mohr-coulomb material model was used to simulate the soil behavior. An idealized soil profile was assumed as given in Table 2, noting that the fill was neglected in this case study. The building was modeled as an isotropic elastic weightless shell with a Young's modulus (E_{eq}) of 1.07GPa, Poisson's ratio of 0.15, and equivalent thickness (t_{eq}) of 16.08m. The tunnel was modeled using isotropic elastic material model with a Young's modulus of 23GPa, Poisson's ratio of 0.2, and shell thickness of 0.4m.

Table 3. Idealized soil profile for the finite difference model.

Layer	Thickness (m)	γ (kN/m^3)	ø	E (MPa)
Upper sand	20	19.5	38	70
Lower sand	40	19.5	38	240

3.1.5 *Finite difference numerical model results*

The predicted and observed responses for the building, along with the finite difference model results are shown in Figure 5. The observed maximum settlement due to tunnel construction was -3.0 mm and the predicted FDM maximum settlement was -4.35mm with an error of 1.35 mm.

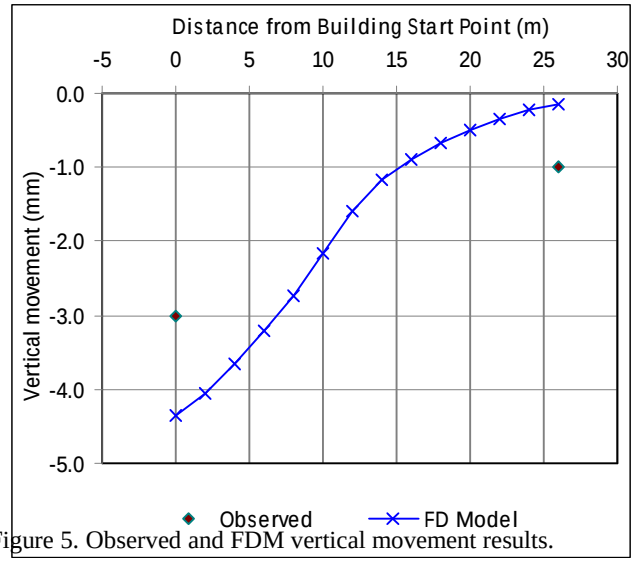

Figure 5. Observed and FDM vertical movement results.

The observed settlement at the end of the building was -1.0mm and the predicted FDM settlement was -0.149mm with an error of 0.851mm on the conservative side. The deviation of the finite difference model results from the observed building settlement is mainly due to the uncertainty of the underground condition below the building and that the measured settlement was only after 20 days from TBM passing. The shape of the model results can't be compared with the observed curve because there was on-

ly two observed points at the east side of the building (**a** and **b** in Fig. 3).

3.2 *Jubilee Line Extension Tunnel case study*

London Jubilee Line Extension tunnel in East London is one of the capital's largest civil engineering projects to date. Its route includes 15.5km of twin bored tunnels and 11 major stations. The behavior of Neptune House in Modkee street was used to verify the proposed finite difference model.

3.2.1*Groundconditions*

Ground conditions at the site consist of 2m of fill overlying 4m of Thames Gravel. The gravel lies on top of the various units of the Lambeth Group, which extends to a depth of 20 to 25m, under which lies a bed of Thanet layer to the top of the Upper Chalk formation at a depth of approximately 40m. The material descriptions and layer depths taken from a borehole located approximately 20m south west of Neptune House (Pickhaver 2006).

3.2.2 *Description of the building*

Neptune House in Moodkee Street, Rotherhithe was used in this study because it almost meet all the the criteria oulined before except its orientation is not perpendicular to tunnel axis. The building is constructed of solid load bearing brick masonry and is three-storey high. The building dimensions are approximately 40m by 8m in plan.

3.2.3 *Finite difference numerical model composition*

Soil was modeled using a mesh dimensions 120m in width, 120m in length and 40m in height (Fig. 6).

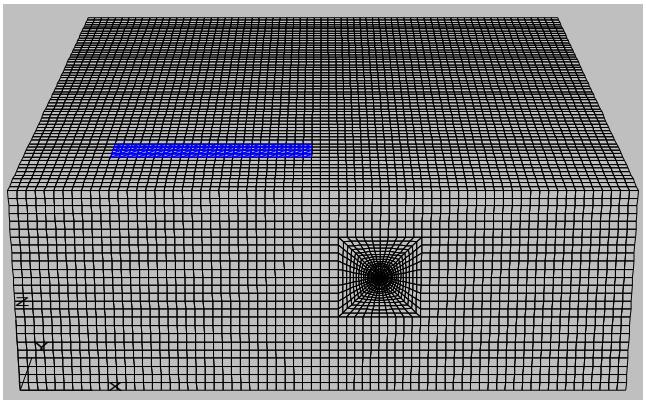

Figure 6. Mesh geometry for Jubilee Line Extension case study

The building was modeled by an elastic weightless shell located on the ground surface. It had a width of 8m , a length of 40m, and a distance of 14m from the tunnel centerline. The building geometry differs from the real building layout; the building is oriented with an angle of 30˚ with the tunnel route. This difference was taken into consideration in the predicted finite difference results by dividing the result value by cosine 30˚. The tunnel was modeled as cylindrical element at depth of 17.0m from ground surface.

Mohr-coulomb material model was used to simulate the soil behavior. For the sake of comparison with the finite element model results conducted by Pickhaver (2006), an idealized soil properties as given by Pickhaver (2006) was taken, and shown in Table 3. The building was modeled as an isotropic elastic weightless shell that has a Young's modulus (E_{eq}) of 1.35GPa, Poisson's ratio of 0.15, and an equivalent thickness (t_{eq}) of 10.2m. The tunnel was modeled using isotropic elastic material model which has a Young's modulus of 23GPa, Poisson's ratio of 0.2, and a shell thickness of 0.25m.

Table 4. Idealized soil profile for the finite difference model.

Layer	Thickness (m)	γ (kN/m^3)	c_u (kPa)	E (MPa)
Lambeth Group	25	20	40	60
Thanet Beds	15	22	210	300

3.2.4 *Finite difference numerical model results*

The finite element predicted response (Pickhaver 2006) and observed responses for Neptune House, along with the finite difference model results are shown in Figure 7.

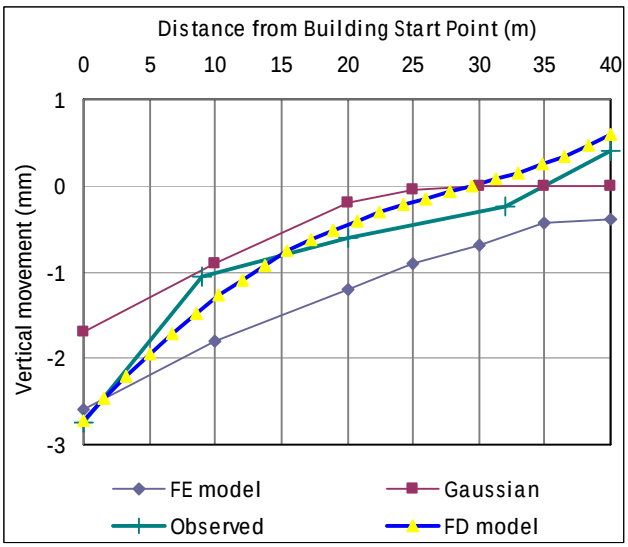

Figure 7. Neptune House FDM results.

The observed response closely matched the predicted response, with negligible building curvatures developing and with very similar maximum settlements. The observed maximum settlement due to tunnel construction was -2.75mm and the

predicted FDM maximum settlement was -2.72mm with an error of 0.03mm with error ratio of 1.09%. The observed settlement at the end of the building was +0.4mm and the predicted FDM settlement was +0.585mm with an error of 0.185mm with error ratio of 39.5%. The shape of the model results is almost the same with the observed curve even for the small upward movement at the end of the building. Figure 7 shows that the proposed finite difference model was predicting the induced building movement with reasonable accuracy.

4 DERIVATION OF MAIN SETTLEMENT CONTROL PARAMETERS

Settlement control parameters are the parameters that govern the response of a building to settlements, namely: vertical movement (S_v), max. vertical movement (S_{max}), max. differential settlement (ΔS_{max}), max. deflection ratio (Δ/L), horizontal movement (S_h), horizontal strain (ε_h), and max. tensile strain ($\varepsilon_{t,max}$). The above control parameters only describe 'in-plane' deformation. Three-dimensional behavior such as twisting is not included in this study.

4.1 *Vertical movement*

FLAC^{3D} is automatically generates the vertical movement (S_v) at any section of the numerical model. Max. (S_{max}) and Min. (S_{min}) vertical movement can be determined by taking the first derivative of the vertical movement curve and equating its value with zero. Practically, the max. settlement due to tunnel construction is above the centerline of the tunnel. Max. differential movement (ΔS_{max}) is the difference between S_{max} and S_{min}. Max. differential movement is crucial than the max. vertical movement because it affects both serviceability and structural performance of the building.

4.2 *Maximum deflection ratio*

For the determination of max. deflection ratio (Δ/L) for hogging or for sagging zone, point of inflection should be located first. Point of inflection is the point separates the hogging zone from the sagging zone in a specific vertical movement curve. Three methods are proposed to locate the point of inflection. The first method is to locate point of inflection by using manual investigation of the vertical movement curve. The second method is to locate point of inflection by empirical correlation between the location of point of inflection and the depth of the tunnel axis (as used by most of researchers). The third method is to locate point of inflection by mathematical formulae that for any polynomial curve, point of inflection is lying at the point where the second derivation of the curve equal to zero. Because of its accuracy, the third method was used throughout this study. After locating point of inflection, width of hogging (L_{hog}) and sagging (L_{sag}) zone can be determined. By dividing the max. differential movement by the corresponding zone width, the max. hogging and sagging deflection ratio ($\Delta/L_{max,hog}$, $\Delta/L_{max,sag}$) can be determined.

4.3 *Horizontal movement*

FLAC^{3D} is automatically generates the horizontal movement (S_h) at any section of the numerical model. Horizontal strain (ε_h) can be determined by taking the first derivative of the horizontal movement.

4.4 *Maximum tensile strain*

Maximum tensile strain ($\varepsilon_{t,max}$) can be determined from the following equations (quoted from Guglielmetti et al. 2008):

$$\varepsilon_{t,max} = \text{max. of } (\varepsilon_{bt}\,;\, \varepsilon_{dt}) \quad (7)$$

$$\varepsilon_{bt} = \varepsilon_h + \varepsilon_{bmax} \quad (8)$$

$$e_{dt} = 0.35e_h + \sqrt{(0.65e_h)^2 + e^2{}_{d\,\max}} \quad (9)$$

where ε_{bt} is the resultant bending tensile strain, ε_{dmax} is the maximum diagonal tensile strain, ε_{dt} is the resultant diagonal tensile strain.

Expressions for ε_{bmax} and ε_{dmax} are derived as functions of the deflection ratio Δ/L (quoted from Guglielmetti et al. 2008) as shown in following equations:

$$\frac{\Delta}{L} = \left\{\frac{L}{12t} + \frac{3I}{2tLH}.\frac{E}{G}\right\} e_{b\,\max} \quad (10)$$

$$\frac{\Delta}{L} = \left\{1 + \frac{HL^2}{18I}.\frac{G}{E}\right\} e_{d\,\max} \quad (11)$$

where L is the building length in hogging or sagging region, H is the thickness of building equivalent shell, t is the distance of extreme fiber in hogging or sagging region (t = H/2 in sagging; t = H in hogging), E and G are the elastic and shear modulus of the building (E/G = 2.6 for masonry buildings), and I is the moment of inertia of equivalent shell (I = $H^3/12$ in sagging; I = $H^3/3$ in hogging). Masonry building damage category is directionally related to maximum tensile strain as stated by Burland et al.

(1977). Their popular table regarding the damage classification for masonry buildings was used in settlement prediction/building damage assessment charts.

5 SETTLEMENT PREDICTION/BUILDING DAMAGE ASSESSMENT CHARTS

Figure 8 demonstrates the parameters used in the derivation of SP/BDA charts and their values.

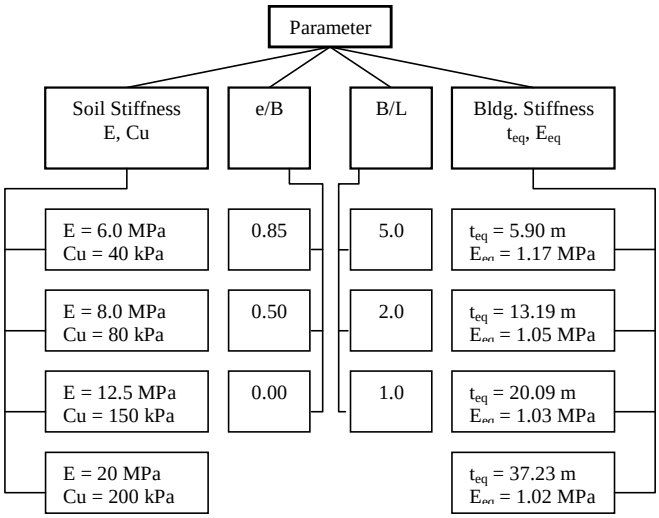

Figure 8. Parameters used for SP/BDA Charts.

5.1 *SP/BDA Charts development assumptions*

The assumptions are: The medium is homogeneous, cohesive soil with unit weight of 20kN/m^3 extending from ground surface to a depth not less than three times the tunnel diameter underneath the center of the tunnel with no ground water exists, the tunnel depth/diameter ratio is constant throughout the length of the building and is equal to 12/4, tunnel lining is rigid enough to withstand the entire applied load without significant deformation, tunneling method is shield method, building consists of reinforced concrete slabs bearing on masonry walls with no existing damage, and the building is oriented perpendicular to the tunnel axis.

5.2 *Procedure for using the SP/BDA Charts*

1) Calculate building eccentricity related to building width ratio (e/B).
2) Calculate building width related to its length ratio (B/L).
3) Using the value for e/B and B/L, choose the most appropriate SP/BDA charts group (ten charts in each group were developed in this research).
4) Calculate building equivalent thickness (t_{eq}) from equations 1 to 6 previously stated.
5) Using t_{eq} on the abscissa, a vertical line intersect the most appropriate soil Young's modulus (E), giving the value of the settlement control parameter in the ordinate corresponding to the intersection point. Ten settlement control parameters and building damage category can be determined from the SP/BDA charts, namely; max. vertical movement, max. differential vertical movement, max. horizontal movement, max. differential horizontal movement, max. hogging and sagging deflection ratio, max. hogging and sagging horizontal strain, max. hogging and sagging tensile strain, and building damage category.

5.3 *SP/BDA Charts*

A sample of the settlement prediction/building damage assessment charts are presented for e/B = 0.5, and B/L = 5.0 (Fig. 9) to determine max. vertical movement (Chart a), max. horizontal movement (Chart b), max. sagging tensile strain (Chart c), max. hogging tensile strain (Chart d), and building damage category (Charts c and d).

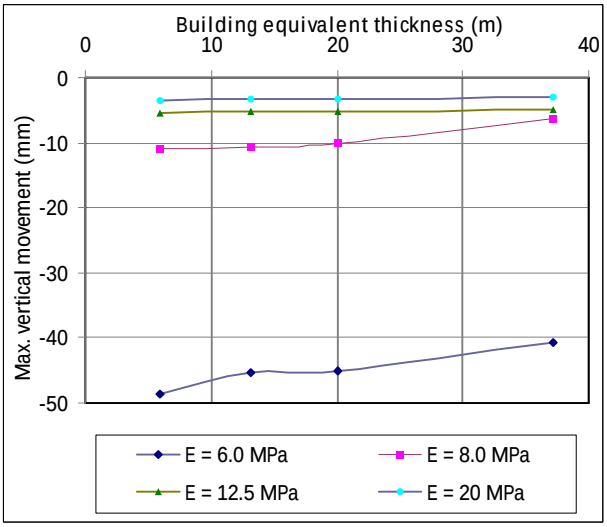

Chart a

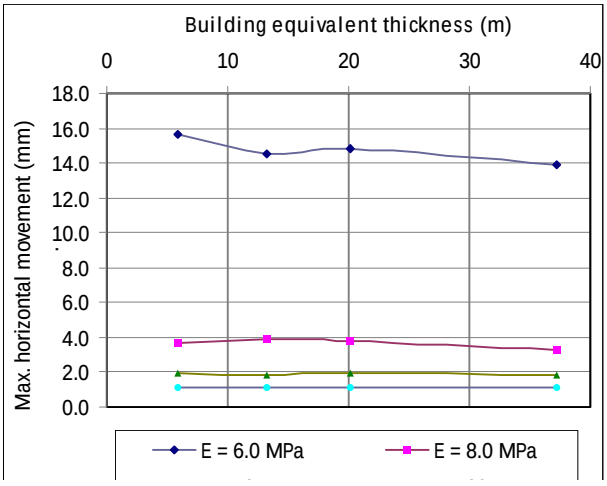

Chart b

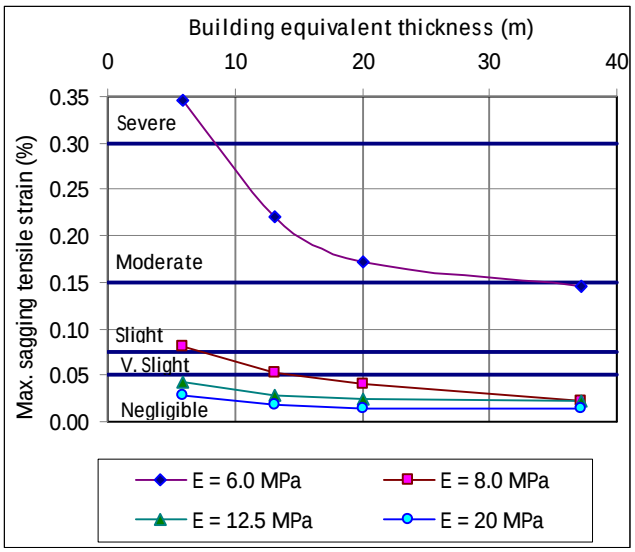

Chart c

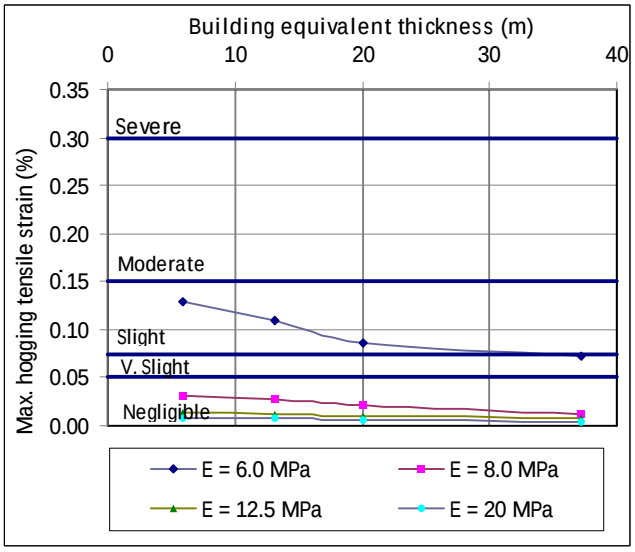

Chart d

Figure 9. SP/BDA Charts

6 SUMMARY AND CONCLUSIONS

A finite difference model (FDM) was used to predict building induced damage due to tunnel construction. The proposed FDM was verified using two cases; a building response due to construction of the Greater Cairo Metro Line 3-Phase 1, and Neptune House response due to construction of the Jubilee Line Extension Tunnel in London. By comparing the FDM predicted response with the observed response for Cairo tunnel, some deviation was found due to the uncertainty of the underground conditions under the building and that the measured settlement was only after 20 days from TBM passing. Comparing the FDM predicted response with the observed response for Neptune House, it was found that the FDM prediction closely matches the observed response. Using the verified FDM, a Settlement Prediction/Building Damage assessment charts were created to preliminary predict building response due to tunnel construction and associated damage. The accuracy of this prediction is based to a great extent on the availability and accuracy of the collected data regarding the ground conditions beneath the concerned building as well as at the corresponding location of the tunnel. However, it must be pointed out that the negligence of the effect of ground water is a major limitation in this study.

REFERENCES

Burland, J.B., Broms, B.B. & De Mello, V.F.B. 1977. Behavior of foundations and structures. State of the art report, Session 2, Proc. 9th Int. Conf. Soil Mechanics and Foundation Eng., Tokyo: 495-546.

Burland, J.B., Standing, J.R. & Jardine, F.M. (eds.) 2001. Building response to tunneling - case studies from the construction of the Jubilee Line extension, London. Volume 1: Projects and Methods and Volume 2: Case Studies. London: Thomas Telford Ltd.

Dias, D., Kastner, R. & Maghazi, M. 2000. Three dimensional simulation of slurry shield tunnelling. Geotechnical Aspects of Underground Construction in Soft Ground, Kusakabe, Fujita and Miyazaki (eds.), Balkema, Rotterdam: 351-356.

Franzius, J.N. 2003. Behavior of buildings due to tunnel induced subsidence. Ph.D. thesis, Imperial College, University of London.

Guglielmetti, V., Grasso. P., Mahtab, A., & Xu, S. 2008. Mechanized Tunnelling in Urban Areas. London: Taylor & Francis Group.

Itasca. 2006. FLAC3D Online Manual. Itasca Consulting Group, inc, Minnesota.

Moller, S.C. 2006. Tunnel induced settlements and structural forces in linings. Ph.D. thesis, Geotechnical Institute, Stuttgart University.

Mair, R.J. & Jardine, F.M. 2001. Tunnelling Methods. Building response to tunnelling – case studies from the construction of the Jubilee Line extension, London. Chapter 10. Burland, J.B., Standing, J.R. & Jardine, F.M. (eds.). London: Thomas Telford Ltd.

National Authority for Tunnels. 2007. Annex 8A Soil Investigation Interpretative Report. National Authority for Tunnels, Cairo.

National Authority for Tunnels. 2009. The Tunnel between Abbasia Station and Apdou Pasha Station Monitoring Measurements Monthly Report. National Authority for Tunnels, Cairo.

Pickhaver, J.A. 2006. Numerical modeling of building response to tunneling. Ph.D. thesis, Balliol College, Oxford University.

Timoshenko, S. 1955. Strength of materials - part 1. London: D van Nostrand Co.